Plasticity of the dopaminergic phenotype and of locomotion in larval zebrafish induced by changes in brain excitability during the embryonic period

Sandrine Bataille, Hadrien Jalaber, Ingrid Colin, Damien Remy, Pierre Affaticati, Cynthia Froc, Philippe Vernier, Michaël Demarque

1 ∴ *Title (50 w)*

2 **Plasticity of the dopaminergic phenotype and of locomotion in**
3 **larval zebrafish induced by changes in brain excitability during**
4 **the embryonic period.**

5

6 *Embryonic excitability modulates differentiation*

7 Sandrine Bataille*[1], Hadrien Jalaber*[1], Ingrid Colin*[1], Damien Remy[1], Pierre Affaticati[2],

8 Cynthia Froc[1], Philippe Vernier[1] and Michaël Demarque**[1].

9 1. Paris Saclay Institute of Neuroscience, (UMR9197) CNRS and Université Paris-

10 Saclay; Avenue de la Terrasse, 91190 Gif-sur-Yvette, France

11 2. TEFOR Paris-Saclay, CNRS UMS2010 / INRAE UMS1451, Université Paris-Saclay,

12 Avenue de la Terrasse, 91190 Gif-sur-Yvette, France

13 *authors contributed equally

14 **Corresponding author

15 ∴ *Corresponding author email address: michael.demarque@cnrs.fr*

16 ∴ *Number of pages: 39*

17 ∴ *Number of figures, tables, multimedia, and 3D models (separately): 6/0/0/0*

18 ∴ *Number of words for abstract, introduction, and discussion: 233/646/1261*

19 ∴ *Conflict of interest statement:* The authors declare no competing financial interests.

ABSTRACT (233/250 w):

During the embryonic period, neuronal communication starts before the establishment of the synapses with forms of neuronal excitability, called here Embryonic Neuronal Excitability (ENE). ENE has been shown to modulate the correct unfolding of development transcriptional programs but the global consequences for the developing organisms are not all understood. Here we monitored calcium transients in zebrafish embryos as a proxy for ENE to assess the efficacy of transient pharmacological treatments able to either increase or decrease ENE. Increasing or decreasing ENE for 24 hour at 2 days post fertilization (dpf) promoted respectively an increase or decrease in the post-mitotic differentiation of the dopamine (DA) neurons in the telencephalon and in the olfactory bulb of zebrafish larvæ at 6 dpf. This plasticity of dopaminergic specification occurs within a stable population of vMAT2 immuno-reactive cells, hence identifying an unanticipated biological marker for this pool of reserve cells, that can be recruited through ENE.

Modulating ENE also affected locomotion several days after the end of the treatments. In particular, the increase of ENE from 2 to 3 dpf promoted an hyperlocomotion in 6 dpf zebrafish larvæ, reminiscent of endophenotypes reported for Attention Deficit with Hyperactivity Disorders and schizophrenia in zebrafish. These results provide a convenient framework to identify environmental factors that could disturb ENE as well as to study the molecular mechanisms linking ENE to the neurotransmitters specification, with clinical relevance for the pathogenesis of neurodevelopmental disorders.

Significance Statement (109/ 120 w):

- Spontaneous calcium spikes, used as a proxy for Embryonic Neuronal Excitability (ENE), are detected in the forebrain of embryonic zebrafish.

- Transients pharmacological treatments applied by balneation could be used to increase or decrease ENE.

- The post-mitotic differentiation of the dopaminergic phenotype is modulated by ENE in the zebrafish forebrain.

- The plasticity of the dopaminergic specification occurs within a reserve pool of vMAT2 immuno-reactive cells.

- Transient increase of ENE at the end of the embryonic period induces a hyperlocomotion, a phenotype associated with ADHD and schizophrenia in this model.

- Our results open clinically relevant perspectives to study the pathogenesis of neurodevelopmental disorders in zebrafish.

Introduction (646/650 w)

During brain development, specific molecular components of the synaptic neuronal communication such as ion channels, neurotransmitters and neurotransmitter receptors are expressed and functional before synapse formation (Spitzer et al., 2002). They contribute to immature forms of cellular excitability and intercellular communications we propose to refer to as Embryonic Neuronal Excitability (ENE). There is for instance a paracrine communication mediated by activation of receptors by endogenous neurotransmitters, GABA and glutamate, in the neonatal rat hippocampus, or glycine in the mouse spinal cord (Demarque et al., 2002; Owens & Kriegstein, 2002; Scain et al., 2010). Acute changes of calcium concentration have also been described, including filopodial or growth cone transients, and calcium spikes

70   in differentiating neurons (Gomez & Spitzer, 1999; Gomez et al., 2001; Borodinsky et

71   al., 2004). Calcium spikes are sporadic, long lasting global increase of intracellular

72   concentration of Ca^{2+} that occurs during restricted developmental windows called

73   "critical periods". They have been identified in the developing brain of several

74   vertebrate species (Owens & Kriegstein, 1998; Borodinsky et al., 2004; Crepel et al.,

75   2007; Blankenship & Feller, 2010; Demarque & Spitzer, 2010; Warp et al., 2012;

76   Plazas et al., 2013). Quantification of calcium spikes by calcium imaging can be used

77   as proxy for ENE. Changes in the incidence and frequency of calcium spikes modulate

78   the specification of the neurotransmitter phenotype in neurons, as it is the case for

79   dopamine (DA), in several cell populations of the xenopus and mouse brain, with

80   consequences on several behaviors (Dulcis & Spitzer, 2008; Dulcis et al., 2013, 2017).

81   DA is an evolutionary conserved monoamine involved in the neuromodulation of

82   numerous brain functions in vertebrates, including motivational processes, executive

83   functions and motor control (Klein et al., 2019). Accordingly, alterations of the

84   differentiation and function of the neurons synthetizing DA contribute to the

85   pathogenesis of several brain disease with a neurodevelopmental origin, such as

86   Attention Deficit Hyperactivity Disorder (ADHD) and schizophrenia (SZ) (Lange et al.,

87   2012; Murray et al., 2017).

88   Further addressing the complex molecular and cellular mechanisms linking

89   developmental excitability, dopaminergic differentiation and behavioral outputs

90   requires an *in vivo* approach in a model accessible, genetically amenable and with

91   possible parallels with the human situations. The developing zebrafish *Brachydanio*

92   *rerio* fits with these needs. The development of the embryos is external, which allows

93   inducing perturbations of ENE at stages that would be *in utero* in mammalian models.

94   The embryos are relatively small and transparent, simplifying high-resolution imaging

95   of the brain in live or fixed preparations. Despite difference in the brain organization,

96   notably a pallium very different form the 6-layered cortex of mammals, the main

97   neuronal systems of vertebrates are present in zebrafish and respond to psychoactive

98   drugs (Gawel et al., 2019). In addition, the monoaminergic system has been

99   extensively studied in zebrafish (Schweitzer & Driever, 2009; Schweitzer et al., 2012).

100   In vertebrates, DA modulates executive functions, such as working memory and

101   decision making, through innervation of specific regions of the telencephalon. In the

102   zebrafish brain, most DA neurons innervating the telencephalon have their cell bodies

103   located within the telencephalon itself (TelDA cells) (Tay et al., 2011; Yamamoto et al.,

104   2011). To the best of our knowledge, there is no evidence for a plasticity of the

105   neurotransmitter phenotype in these cells.

106   To perturb ENE in conditions close to physiological exposure and ecotoxicology,

107   we used pharmacological treatments by balneation from 48 to 72 hours post

108   fertilization (hpf). We then analyzed the consequences of these transient

109   pharmacological treatments a few days later, between 6 and 7 dpf. We report

110   quantifiable changes in the specification of the dopaminergic phenotype in TelDA

111   neurons. We also report changes for high-speed swimming episodes. These results

112   suggest a role of ENE on the specification of the dopaminergic phenotype and motor

113   control in the zebrafish. They also open important perspectives for this model to

114   decipher the chain of events leading from environmental factors to the pathogenesis

115   of disorders such as schizophrenia and ADHD.

116

117 **Materials and Methods**

118 **Fish strains**

119 All experiments were carried out in accordance with animal care guidelines

120 provided by the French ethical committee and under the supervision of authorized

121 investigators.

122 Zebrafish were raised according to standards procedures. Briefly, for breeding,

123 males and females zebrafish were placed overnight, in different compartments of a

124 tank with a grid at the bottom that allows the eggs to fall through. The next morning the

125 separation was removed and after few minutes, the eggs were collected, rinsed and

126 placed in a petri dish containing embryo medium (EM). Embryos were kept at

127 28 degrees, then staged as hours post fertilization according to specific criteria. The

128 number of animal used for each experiments is indicated in the corresponding figure

129 legends.

130 **Pharmacological treatments**

131 Pharmacological compound, veratridine (10 µM), TTX (2 µM), ω conotoxin

132 (0.08 µM), nifedipine (0.4 µM) and flunarizine (2 µM) were purchased form R&D

133 System (UK) and prepared in water except veratridine which required dimethyl

134 sulfoxide (DMSO) for dissolution and flunarizine that requires ethanol for dissolution.

135 Sham control were performed using the same concentration of DMSO in EM without

136 the drug to rule out an effect of the detergent itself. Specific period and duration of

137 applications are indicated in the corresponding figure legends. All pharmacological

138 treatments were performed by balneation followed by three washes in EM. Embryos

139 were randomly distributed in wells (30 embryos per well) of a 6-well plate containing

140 5 mL of solution (EM+DMSO or EM+drug). Embryos exposed to drugs or the sham

141 control solution were observed for morphological abnormalities every day until 5 dpf.

142   Malformations (*e.g.* spinal curvature, cardiac edema) were considered as experimental

143   end-points and when detected the corresponding animals were excluded from the

144   study.

145   **Calcium imaging**

146   At 24 hpf embryos of the (Hsp70:GAl4 x UAS:GCaMP6f;cry:mCherry) line were

147   exposed to a 38°C temperature for 1.5 hour. Upon heat shock activation, GCamp6f is

148   expressed in all the cells of the animals.

149   At 2-3 dpf the embryos were then individually embedded in low melting agarose,

150   ventral side up for imaging.

151   30 min time lapse series were acquired at 1 Hz, at a single focal plane, on an

152   Olympus BX60 microscope (Olympus corporation, Tokyo, Japan) equipped with a

153   40x 0.6N water immersion objective. A non-laser spinning disk system (DSD2, ANDOR

154   Technology, Oxford, UK) was used for illumination and image acquisition. Images were

155   open in Fiji and analyzed using Multi Measure (W. Rasband, B. Dougherty), Measure

156   Stack (Optinav, Redmond, WA), and custom Image J plugins. Regions of interest

157   (ROIs) were drawn manually over individual cell bodies. Movements of the preparation

158   in the X/Y axis were corrected using the plugin Measure Stack. Average gray level

159   from pixels in ROIs was measured over time. Spikes were defined as increase of

160   fluorescence higher than 2 times the standard deviation of the baseline. The duration

161   of spikes was calculated as the width at half-maximum. Incidence was scored as the

162   number of cells generating transients divided by the estimated total number of cells in

163   the imaged field and was expressed as a percentage. Frequency was calculated as

164   the total number of transients in a given cell divided by the total acquisition time and

165   was expressed as spikes per hour.

Immunohistochemistry

Tissue preparations

6-7 dpf zebrafish larvæ were deeply anesthetized using 0.2% Ethyl3-amniobenzoate methanesulfonate (MS222; Sigma-Aldrich) diluted in EM, then they were fixed in ice-cold 4% paraformaldehyde (PFA; Electron Microscopy Sciences) in 1X phosphate-buffered saline (PBS; Fisher Scientific) containing 0.1% Tween 20 % (PBST) overnight at 4 °C. Samples were dehydrated and stored in MeOH at -20°C.

Immunofluorescence

Immunofluorescence was performed in 2 mL microtubes. Unless specified otherwise in the protocol, incubations were performed at room temperature (RT), and thorough PBST washes were performed between each steps. The samples were first incubated in 3% Hydrogen Peroxide Solution (H_2O_2) in Ethanol 100% (EtOH) for 30 minutes, to deactivate endogenous peroxidases. They were then successively incubated in EtOH:Xylen 1:1 without agitation for 1 hour and, at -20 °C, in EtOH:Aceton 1:2 without agitation for 20 minutes. The washes were performed between these steps were performed in EtOH. After the final wash, samples were rehydrated in PBST.

In order to unmask the antigens, samples were incubated in PBST:Tris 150 mM pH9 for 10 minutes, then in Tris 150 mM pH9 at RT for 10 minutes and at 70 °C for 30 minutes. After PBST washes, the samples were incubated in a blocking buffer (10% normal goat serum (NGS), 1% triton X-100, 1% tween-20, 1% DMSO, 1% Bovin Serum Albumin (BSA) in PBS 1X) for 3 hours.

Two protocols were used for primary antibody staining. For the TH antibody, the samples were incubated with the first primary antibody (mouse anti-TH, 1:250) in a staining solution (1% NGS, 1% triton X-100, 1% DMSO, 1% BSA, 0,05% azide sodium

191   in PBST) at 4°C for 7-10 days, under gentle agitation. The samples were then

192   incubated in a blocking buffer DAB (4% NGS, 0,3% triton X-100, 0,5% DMSO in PBST)

193   for 1 hour at RT and incubated with a first secondary antibody (anti-mouse biotinylated,

194   1:200) in a secondary staining buffer (4%NGS, 0,1% triton X-100 in PBST) for 2,5 days

195   at 4°C under gentle agitation.

196   For the revelation, we used the Vectastain ABC kit (Vector ®).Briefly, a AB mix

197   was prepare by adding 10 µl of solution A and 10 µl of solution B in 1mL PBST/1%

198   Triton-X100. One hour after the preparation, the samples were incubated in the AB mix

199   for 1 hour. Samples were then incubated in Tyramid-TAMRA (1:200 in PBST) for

200   20 minutes, then 0,012% H_2O_2 was added directly in the solution and the samples

201   were incubated for an additional 50 minutes.

202   Before a second primary antibody incubation, the samples underwent a step of fixation

203   in PFA 4% for 2 hours at RT and washed overnight in PBST.

204   For the other primary antibodies (rabbit anti-caspase3, 1:500 or chicken anti-GFP,

205   1:500), the samples were incubated in the blocking buffer (1 hour when following a TH

206   staining, 3 hours otherwise), then they were incubated with the primary antibody in a

207   staining solution at 4 °C for 3-4 days, under gentle agitation. After washes, the samples

208   were incubated with the second secondary antibody (goat anti-chicken Alexa Fluor

209   488, 1:500) and DAPI 1X in PBST at 4 °C for 2,5 days under gentle agitation. Samples

210   were then washed three times in PBST and left overnight in PBST. For observation,

211   the brain were dissected and mounted between slides and coverslides in Vectashield

212   solution (Vector®).

213   *Image acquisition*

214   A Leica TCS SP8 laser scanning confocal microscope with a Leica HCTL Apo

215   × 40/1.1 w objective was used to image the specimens.

216   Fluorescence signal was detected through laser excitation of fluorophores at 405, 488,

217   552, or 638 nm and detection was performed by two internal photomultipliers. Steps in

218   the Z-axis were fixed at 1 μm. Acquired images were adjusted for brightness and

219   contrast using ImageJ/FIJI software.

220   *Quantification of immuno-reactive cells*

221   The TH- and GFP-IR cells were counted manually from z-stacks of confocal

222   images using the ImageJ cell counter plugin.

223   **Spontaneous locomotion assays**

224   Individual larvæ were placed in a well of a 24 well plate with 2 mL EM 2 hours

225   before recordings for habituation. The plate is then placed in a Zebrabox (Viewpoint,

226   Lyon, France) for 10 minutes recording sessions. Locomotor activity was recorded

227   using ZebraLab software (Videotrack; ViewPoint Life Sciences, France). After a first

228   session without threshold for 24 untreated larvæ the average speed (av_sp) of the

229   batch was extracted from the data. For subsequent sessions, two threshold were

230   applied. Swim bouts with a speed below half the average speed (av_sp/2) were

231   considered as inactivity, episodes with a speed over twice the average speed

232   (av_sp*2) were considered as fast episode or burst and episodes with a speed

233   between the two threshold were considered as cruises episodes or normal swim.

234   For each sessions, each animal and each category of episodes (inactivity, cruises

235   epiosdes and bursts episodes), 4 parameters are extracted from the recordings: the

236 number of episodes, the total distance covered, the duration of activity, and the

237 average speed.

Experimental design

Statistical analyses

240   Results are shown as means ± SEM. Means comparisons were performed using

241 the appropriate non parametric statistical tests (ANVOA, Mann Whitney U test or

242 Kruskal-Wallis test depending on the experimental conditions). P < 0.05 was

243 considered statistically significant and noted as follow: P < 0.05 (*), P < 0.01 (**),

244 P < 0.001 (***).

245   For percentages, we used the 95% confidence interval defined as

246 =1.96*squareroot((x*(1-x)/n)), n being the number of independent samples and x being

247 the % of change observed.

248 All statistical tests were performed using the online software Brightstat and R.

Results

Presence of calcium spikes in the brain of zebrafish embryo.

251   To study Embryonic Neuronal Excitability (ENE) in the embryonic zebrafish brain,

252 we recorded calcium spikes as a proxy. To follow the dynamics of intracellular calcium

253 concentration we used the (Hsp70:GAl4 x UAS:GCaMP6f;cry:mCherry) transgenic

254 line, in which the genetically encoded calcium reporter GCamp is expressed upon heat

255 shock activation (see Materials and Methods). To monitor changes in fluorescence

256 over time, we performed time-lapse imaging of the anterior most part of the brain of 2-

257 3 dpf zebrafish embryos for 30 minutes sessions.

258   Spontaneous changes in fluorescence were detected in forebrain cells, likely

259   including presumptive dopaminergic cells in the telencephalon and the OB (Figure 1A).

260   We analyzed the evolution of the fluorescence from selected regions of interest

261   corresponding to individual cell bodies (Figure 1B and Materials and methods). The

262   average frequency of the recorded Ca^{2+} spikes was 6.6+/-5.4 spikes.h-1; the average

263   incidence of these events was 45.2+/-9.7%; these events had a mean duration of

264   3.3/+- 1.6 s (n= 28 spikes from 5 independent preparations Figure 1C, blue boxplots).

265   These parameters are in the range of what has been reported in the zebrafish spinal

266   cord, confirming that the duration of Ca^{2+} spikes is shorter in zebrafish than in xenopus

267   (Dulcis & Spitzer, 2008; Warp et al., 2012; Plazas et al., 2013).

268   **Global pharmacological modifications of calcium spikes dynamics**

269   In order to assess the effects of global manipulations of ENE, we applied

270   pharmacological compounds directly in the embryo medium. The treatments were

271   performed during the last day of embryonic development (48-72 hpf) to reduce the

272   effects on early developmental steps such as neurulation and proliferation. These

273   drugs were already used in *Xenopus* for similar purposes (Borodinsky et al., 2004). To

274   increase calcium spiking we used veratridine (10 µM), which blocks the inactivation of

275   voltage-dependent sodium channels. To decrease calcium spiking, we used a cocktail

276   containing TTX (2 µM), ω-Conotoxin (0.08 µM), Nifedipine (0.4 µM) and Flunarizine

277   (2 µM) targeting respectively voltage-dependent sodium channels; N, L and T subtypes

278   of voltage dependent calcium channels (we refer to this cocktail as TCNF based on

279   the initials of its 4 components).

280   We   performed   time-lapse   recordings   of   the   (Hsp70:GAl4   x

281   UAS:GCaMP6f;cry:mCherry) transgenic line two to ten hours after the beginning of the

282   treatments.

283   Following either veratridine treatment (n=26 spikes from 4 independent

284   preparations) or TCNF treatment (n=15 from 4 independent preparations), individual

285   events had a similar duration as in control (Kruskal-Wallis test, p=0.538; Figure 1C).

286   Following veratridine treatments, the average frequency of calcium spikes was

287   increased (+39.3+/-16%, n=36 cells from 4 independent preparations, p=0.206

288   bonferroni post-hoc test) as well as the average incidence of calcium transients

289   (29.9+/-45% n=4 independent preparations, p<0.05 conover posthoc comparisons;

290   Figure 1C, green boxplots).

291   Following TCNF treatments, the average frequency of calcium spikes was

292   decreased (-29+/-22%, n=17 cells from 4 independent preparations, p=0.812

293   bonferroni post-hoc test) as well as the average incidence (-44+-/48% n=4

294   independent preparations, p<0.01 Kruskal-Wallis paired comparisons)(Figure 1C, red

295   boxplots).

296   These results demonstrate that balneation treatments are able to change the

297   incidence and frequency of spontaneous calcium spikes in the embryonic zebrafish

298   forebrain. Based on these results, we refer to veratridine treatment as "increase of

299   ENE", and to TCNF treatment as "decrease of ENE", in the following sections of the

300   manuscript.

301   **Dopaminergic cells in the telencephalon and the olfactory bulb (OB) in the**

302   **zebrafish brain at larval stages.**

303   To identify dopaminergic neurons in the telencephalon and the OB, we used two

304   markers of the catecholaminergic phenotype, immune-labeled tyrosine hydroxylase 1

305   (TH1), the rate limiting enzyme for dopamine synthesis and the vesicular monoamines

306   transporter (vMAT2) combined to anatomical landmarks such as the position of brain

307 ventricles or large fibers bundles. Indeed, in zebrafish, like in mammals, noradrenaline-

308 containing neuronal soma are not detected in the forebrain anterior to the midbrain-

309 hindbrain boundary, rather, they are restricted to neuronal subpopulations located in

310 the nucleus locus coeruleus, the medulla oblongata and the area postrema (Ma,

311 1994a; b, 1997, 2003). Thus, all the catecholaminergic neurons located in front of the

312 midbrain-hindbrain boundary are likely to be dopamine neurons.

313 To localize these markers we performed double wholemount

314 immunohistochemistry on 6-7 dpf larvæ of the Tg(Et.vMAT2:eGFP) transgenic line.

315 We used an anti-GFP antibody to amplify the endogenous GFP signal to visualize cells

316 expressing vMAT2 (referred to as vMAT2+ cells in the remaining of the manuscript)

317 and an anti-TH antibody to identify TH1 cells (referred to as TH1+ cells in the remaining

318 of the manuscript). This anti-TH antibody is specific to TH1 and does not have affinity

319 for TH2 (Yamamoto et al., 2011).

320 In control conditions, in the telencephalon, we detected 15.1+/-3.1 TH1+ cells

321 (n= 39 samples from 6 independent experiments; Figure 2A, left column, Figure 2B,

322 blue boxplot). The cell bodies of these neurons were distributed bilaterally along the

323 midline, and relatively close to it. The major pattern of fibers distribution we could detect

324 was that of fibers projecting first ventrally and then laterally joining the wide

325 dopaminergic lateral longitudinal tracts.

326 An average of 63.4+/-6.7 vMAT2+ cells was also detected in this region (n= 39

327 samples from 6 independent experiments; Figure 2A, blue boxed column, Figure 2 C

328 blue boxplot). The overall disposition of the cell bodies and projections was the same

329 as for TH+ cells.

330   In control conditions, in the OB, 46.4+/-8.1 vMAT2+ cells and 30+/-2.6 TH1+ cells

331   were detected (n= 39 samples from 6 independent experiments; Figure 2A, blue boxed

332   column and Figure 2D and 2E, blue boxplot). The cell bodies of these OB TH1+

333   neurons were distributed at the anterior end of the forebrain and they were initially

334   projecting in an anterior direction before rapidly branching in multiple directions.

335   In both regions, all TH1+ cells were also vMAT2+ while some vMAT2+ cells were

336   TH1-. In the telencephalon, vMAT2+/TH1- cell bodies were mostly located at the

337   anterior end of the cluster of vMAT2/TH1+ cells. Such vMAT2$^+$/TH$^-$ cells are also

338   detected in the telencephalon of adult zebrafish (Yamamoto et al., 2011). Thus, in the

339   developing zebrafish telencephalon, the population of vMAT2$^+$ cells slightly exceeds

340   that of TH1-expressing cells.

341   **Effects of pharmacological treatments on the expression of dopaminergic**

342   **markers in the telencephalon and the OB.**

343   To assess the effects of ENE on the expression of telencephalic dopaminergic

344   markers at larval stages, we applied pharmacological treatments by balneation from

345   48 to 72 hpf as described above and performed whole-mount immunohistochemistry

346   on larvæ fixed at 6-7 dpf.

347   Increasing the excitability in the zebrafish brain also increased the number of TH1+

348   cells both in the telencephalon and in the OB (+28.6+/-15%, p<0.05 and +45.9+/-17%

349   p<0.001 respectively, n=35 samples from 6 independent experiments, conover

350   posthoc comparisons, Figure 2A, green boxed column; Figure 2B and 2D, green

351   boxplots). Meanwhile, the number of vMAT2 cells did not change significantly in either

352   regions (p=0.08 for the telencephalon, p=0.659 for the OB, Kruskal wallis test; n=16

353   samples from 6 independent experiments; Figure 2A, green boxed column, Figure

354   2C,E, green boxplots).

355   Following decreased excitability, the number of TH1+ cells diminished in the

356   telencephalon but not in the OB (-14.5+/-9.6% and -0.7+/-7.3% respectively, n=49

357   samples from 6 independent experiments; p<0.001 and p>0.05 respectively, conover

358   posthoc comparisons, Figure 2A, red boxed column, Figure 2B and 2D, red boxplot).

359   Meanwhile, the number of vMAT2 cells did not change significantly in either regions

360   (Kruskal wallis test: p=0.08 for the OB, p=0.659 for the OB; n=24 from 6 independent

361   experiments; Figure 2A, red boxed column and Figure 2C and 2E, red boxplots). In

362   both experimental situations, that is, after increasing or decreasing ENE, all the TH1+

363   cells also exhibited vMAT2 labelling. Hence, according to our identification criteria

364   (anatomical position combined to the expression of TH and vMAT2), an increase of

365   embryonic electrical activity increases the number of TelDA cells, while a decrease of

366   embryonic electrical activity decreases the number of TelDA cells.

367   On the other hand, the number of vMAT2+ cells was relatively stable in comparison

368   to TH1+ cells following the perturbation of activity (only decreasing in the telencephalon

369   following a decrease of activity). The stability of the number of vMAT2+ cells and the

370   lower proportion of vMAT2$^+$/TH$^-$ cells following increase of ENE suggest that the cells

371   that express a complete dopaminergic phenotype in this condition are recruited among

372   a population of vMAT2$^+$/TH$^-$ cells. Hence vMAT2$^+$/TH$^-$ cells would behave as a reserve

373   pool for dopaminergic cells (Dulcis & Spitzer, 2012). A similar conclusion could also

374   apply to the OB, despite the fact that the number of TH1+ cells is not statistically

375   diminished following decreased activity in this region. This unexpected result could

376   account for a number of TH1+ cells already set at a minimum in basal conditions in the

377   OB.

378   **Modifications of ENE do not have an effect on cell death in the forebrain**

379   To check whether increase or decrease of ENE could change cell survival, we

380 counted the number of cells IR for the apoptosis marker caspase-3 at 6-7 dpf. The

381 number of caspase-3+ cells was stable following the increase or the decrease of ENE,

382 strengthening the hypothesis that the changes observed in the number of TH1+ cells

383 is indeed linked to changes in specification rather than changes in cell death (Figure 3).

384 **Maturation of spontaneous swimming in zebrafish larvæ**

385   In order to analyze the consequence of changes in ENE on motor behaviors in

386 zebrafish larvæ, we recorded swimming episodes, as described in Materials and

387 Methods. During locomotion, zebrafish larvæ display successive turn and swim bouts

388 called episodes, interleaved with resting periods. This behavior can be analyzed by

389 semi-automated methods, making possible to distinguish between episodes based on

390 the average swim speed. Swimming episodes with a speed close to the overall average

391 speed of all recorded episodes are considered as cruises episodes or normal swim.

392 Episodes with a speed higher than twice the overall average speed of all recorded

393 swim episodes, are considered as fast episodes or bursts.

394   We first studied the dynamic of maturation of larval cruises and bursts episodes in

395 control conditions. We tracked the position of individual larvæ during 3 rounds of

396 10 minutes recordings at 4, 5, 6 and 7 dpf. The recorded parameters reflected a

397 gradual increase of spontaneous locomotion from 4 to 6 dpf and a relative stability

398 between 6 and 7dpf. From 4 to 6 dpf, the number of episodes, the duration of swimming

399 and distance covered increases, both for cruises and bursts episodes ($p<0.01$ for each

400 parameters, Bonferroni post-hoc test, n=48 individuals for each stages; Figure 4,

401 lighter blue boxplots). In contrast, between 6 and 7 dpf, the recorded parameters were

402 stable both for cruises and bursts episodes ($p=0.16$, 1 and 1 respectively; Figure 4,

403 darker blue boxplots). Based on these results, we concluded that we could set our

404 analysis window between 6 and 7 dpf.

Effects of pharmacological treatments on the locomotion of 6-7 dpf larvæ.

We next studied the effect of transient increase and decrease of ENE during the embryonic period on locomotion recorded in larval zebrafish (Figure 5A). We recorded spontaneous locomotion of 6-7 dpf zebrafish larvæ over 3 consecutive 10 minutes sessions in 3 conditions: control, increased ENE, and decreased ENE. A representative example of traces obtained for 24 well plates for each conditions is shown in Figure 5B. For cruises and bursts episodes, the four parameters measured were the number of swim bouts, the total duration of swim, the total distance covered, the average speed of swim (Figure 5 C-J).

For cruises episodes, in control conditions, the four measured parameters were the number of swim bouts: 1267.2+/-292.3, total duration: 306.5+/-58.6 s, total distance covered: 767.5+/-285.1 mm and average speed: 2.5+/-0.7 mm.s^{-1} (n=318 larvæ from 15 independent experiments, Figure 5B-F, blue boxplots).

The number of swim bouts was decreased following both the increase and the decrease of ENE (-5.8+/-2.3% ; -22+/-5% respectively, Figure 5C). The three other parameters increased either after an increase or a decrease of ENE (the total duration: +4.6+/-2.1% ; +35.4+/-5.8%; the total distance covered: +38.3+/-4.9% ; +14.7+/-4.3% and average speed: +34,6+/-4.8% ; +22.2+/-5% respectively, p<0.01 conover posthoc comparisons; n>262 larvæ from 15 independent experiments; Figure 5D-F).

For bursts episodes, in control conditions, the 4 parameters studied were the number of swim bouts: 301+/-227.6, the total duration: 42+/-38.4 s, the total distance covered: 434.2+/-492.6 mm and the average speed of swim: 9.7+/-2.8 mm.s^{-1} (Figure 5 G-J, blue boxplots).

428   Three of these parameters changed according to the treatments. They increased

429   following an increase of ENE and decreased following a decrease of ENE (number of

430   swim bouts: +24.6+/-4%;-54.8+/-6%; total duration: +37.8+/-4.8%;-58+/-6%; total

431   distance covered: +58.8+/-5%;-61.6+/-5.9% respectively, % of change followed by the

432   confidence interval, n>262 larvæ from 15 independent experiments; p<0.01 conover

433   posthoc comparisons, Figure 5G-J). Average speed also increased following a

434   increase of ENE (+17+/-3.8% Figure 5J, green boxplot) while it did not change

435   following a decrease of ENE (Figure 5J, red boxplot).

436   These results showed that the consequences of perturbing the embryonic

437   electrical excitability are different on the cruises episodes and on bursts episodes,

438   suggesting that the underlying neural networks of these swimming modes are not the

439   same and/or that they are not regulated in the same way following changes in ENE.

440   **Kinetics of the direct effects of acute pharmacological treatments on the**

441   **locomotion of 6-7 dpf larvæ.**

442   To exclude a direct effect of the drugs used on the larvæ locomotion, we next

443   followed the time course of the effects of acute pharmacological treatments (veratridine

444   and TCNF) in 6-7 dpf larvæ. We performed 10 minutes recording sessions before

445   application of the treatments, then +2 hours, and 24 hours after the treatments.

446   For cruises episodes, the results obtained following acute veratridine applications

447   are close from the one induced by the embryonic applications with a decrease of the

448   number of episodes and an increase of the duration and the distance. Only the results

449   for the average speed are different since it was not significantly different following acute

450   application while it increased following embryonic application (Figure 6A-D green

451   boxplots). Following T.C.N.F applications the number of events decreased like similarly

452 as following embryonic application while duration, distance and average speed

453 remained unchanged (Figure 6A-D red boxplots).

454 For bursts episodes, acute treatments had overall similar effects on the recorded

455 parameters as the one recorded after treatments performed in 2-3 dpf embryos (Figure

456 6). Veratridine application induced an increase of duration and distance, while the

457 number of events and the average speed were not significantly different (Figure 6E-H

458 green boxplots). T.C.N.F application led to a decrease of number of events, duration

459 and distance during bursts, only the average speed remained unchanged

460 (Figure 6E- H red boxplots).

461 By the next day, while some of the effects of the acute treatments are still

462 detectable, all the effects of these treatments on bursts episodes had faded away

463 (Figure 6E-H, lighter colored boxplots). These results clearly show that the delay

464 between the embryonic treatments and our analysis of larval locomotion is longer than

465 the time required for the disappearance of the acute effect of the drugs. Hence, these

466 results support the existence of a long-term effect related to changes in electrical

467 activity during the embryonic period in the zebrafish.

Discussion (1261 / 1500w)

Summary

Immature forms of excitability, referred to here as Embryonic Neuronal Excitability (ENE), including calcium spikes and activation of non-synaptic receptors to neurotransmitters, contribute to modulate neuronal differentiation. Here we show that the developing zebrafish is a suitable model to manipulate ENE using pharmacological treatments and to study the consequences of these manipulations on the plasticity of neuromodulator systems, at works in the pathogenesis of several human neuropsychiatric diseases. Indeed, we report that ENE exerts a positive regulatory effect on the specification of the dopaminergic phenotype by increasing the number of dopamine cells in the telencephalon. The pharmacological manipulation of ENE has also a clear behavioral outcome by changing the occurrence of high-speed episodes of swimming in zebrafish larvæ.

Balneation treatments and ENE

For the present study, zebrafish embryos were exposed to pharmacological compounds by means of balneation treatments. This methodological approach allows performing global and transient drugs applications, relevant to natural situations where embryos can be exposed to various biologically active or toxic compounds. Zebrafish is highly suitable for such questions because of its external development in an egg, and because its blood brain barrier is not fully mature until 10 dpf, allowing diffusion of the drugs to the neuronal tissues. As a consequence, we were able to analyze alterations by pharmacological treatments of calcium transients, one of the main form of immature excitability.

We focused on calcium transients to assess the effectiveness of the treatments, but other intercellular communication processes such as the paracrine activation of GABA

493 and glutamate receptors by endogenous transmitters are also likely perturbed by the

494 treatments. Further studies are required to decipher the specific contribution of each

495 of these mechanisms to the cellular and behavioral effects we reported here.

496 *Calcium transients in the zebrafish forebrain*

497 One reason to focus on calcium transients is that they have been involved in

498 neurotransmitter phenotype specification in other models of neuronal plasticity. In

499 addition, calcium transients are conveniently measured by calcium imaging.

500 Calcium transients were already reported in the spinal cord of zebrafish embryos

501 around 24 hpf. Here, recordings were performed in the forebrain of embryonic

502 zebrafish around 48 hpf, a time at which the transition toward synaptic network activity

503 has occurred in the spinal cord. These observations are in accordance with the

504 existence of an postero-anterior gradient of neuronal maturation, similar to what was

505 described in xenopus.

506 Calcium transients in the forebrain had frequency and duration similar to what has

507 been described in the zebrafish spinal cord. This duration is overall shorter than what

508 has been observed in the Xenopus nervous system. The basis of these interspecies

509 differences are not known, but it suggests that the duration of the transients is not

510 necessarily the pertinent signal to trigger the effect on neuronal differentiation. This is

511 further suggested by the results of the TCNF treatments reported here, which lead to

512 changes in DA specification and in locomotion parameters, while the duration of

513 individual spikes duration was not changed.

514 We chose to drive the expression of GCamp by an exogenous trigger, here a heat-

515 shock. This allowed the expression of the calcium reporter in all the cells present at

516 the selected period of recordings. The next step of our approach will thus be to use

517 differentiation markers of the DA lineage to identify the differentiation status of the cells

518 where the Ca^{2+} spikes are detected, and also to see whether there are different

519 dynamics of the calcium transients between different subregions of interest in the

520 embryonic brain by using whole brain calcium imaging.

521 *Identification of a biomarker for DA reserve pool neurons?*

522 The effect of ENE perturbations on the DA phenotype analyzed by the number of

523 TH1+ cells was in agreement with the homeostatic rule described in xenopus. Indeed,

524 DA phenotype was enhanced by increased excitability, as expected from an overall

525 inhibitory neurotransmitter. The relative constancy of the number of vMAT2+ cells,

526 together with the absence of significant change is caspase 3-labelled cells upon

527 treatments, suggest that modulation of excitability did not affect cell death or

528 proliferation, but rather triggered a plasticity of the dopaminergic phenotype. This

529 plasticity of the DA phenotype is likely to occur within the pool of vMAT2+ cells, since

530 the number of VMAT2+/TH+ was increased with increased excitability, at the expense

531 of VMAT2+/TH- cells. Therefore, the VMAT2+/TH- cells would be a reserve pool of

532 cells primed to become dopamine neurons when plasticity-triggering events occur.

533 Although somewhat peculiar at first sight, the expression of the vesicular transporter

534 in a reserve pools of cells, might have a functional advantage in term of response to

535 plasticity-triggering events, limiting the number of factors to be changed for reaching a

536 fully functional dopamine phenotype.

537 *Behavioral consequences of ENE*

538 Perturbations of ENE had also behavioral consequences in zebrafish larvæ. For

539 bursts episodes, the initiation of movement is likely to be the prime parameter modified

540 following ENE perturbations. Interestingly, hyperlocomotion is an endophenotype

541 related to ADHD and schizophrenia in zebrafish (Blin et al., 2008; Lange et al., 2018).

542 Determining whether a direct activation of TelDA cells could trigger an increase of

543   bursts episodes is an interesting perspective for the future, as seeing whether other

544   behaviors related to ADHD and schizophrenia such as prepulse inhibition are also

545   affected by alterations of ENE.

546   *Critical period for the effect of ENE perturbations*

547   We observed an effect of the pharmacological treatments performed during the

548   embryonic period on spontaneous locomotion several days after the end of the

549   treatments. In contrast, no effects were observed 24 hours after treatments performed

550   at 6 dpf in the zebrafish larvæ. These long-lasting effects of treatments at specific

551   embryonic time are in line with the existence of a critical developmental period, more

552   sensitive to homeostatic perturbations, promoting therefore significant phenotypic

553   plasticity in immature neurons. Interestingly, dopaminergic systems have multiple

554   functional role and are particularly prone to plasticity events, suggesting that these

555   systems might be a key factor for adaptability of the animals to environmental changes.

556   Whether it is a cause, a consequence or a simple correlation of their conservation

557   throughout animal evolution is still an open question.

558   *Potential involvement of changes of ENE in the pathogenesis of brain disease*

559   According to the 'Developmental Origins of Health and Disease (DOHaD)

560   hypothesis, transient exposure to perturbations during the development could lead to

561   emergence of disease in young or adult individuals (Mandy & Nyirenda, 2018).

562   Neurological and psychiatric diseases, such as autism spectrum disorders, ADHD, or

563   schizophrenia are hypothesized to have a developmental origin. The environmental

564   factors potentially contributing to these pathologies include malnutrition, stress, and

565   drugs exposure during the embryonic period.

566   Results from epidemiological studies and experiments in rodents further suggest

567   that a range of functional and behavioral abnormalities observed in the mature system

568 result from early alterations of dopaminergic neurons differentiation. The data

569 presented here point to an implication of ENE in the regulation of dopaminergic

570 differentiation in the developing brain, suggesting that ENE could act as an

571 intermediate between environmental factors and the molecular changes leading to the

572 alteration of dopamine-related behaviors.

573 These results provide a firm basis to dissect further the cellular and molecular

574 mechanisms linking exposure to external challenges with the subsequent changes in

575 ENE, in the maturation of the dopaminergic systems and its behavioral outputs. A

576 comparative study of the transcription factors differentially expressed in vMAT2 cells

577 following changes in ENE, would help identify dopaminergic related factors having an

578 activity-dependent expression, including epigenetic effectors (level of methylation,

579 histone acetylation).

580 Such mechanisms are underlying phenotypes related to ADHD and schizophrenia

581 in zebrafish, and opens new avenues to better understand how environmental factors

582 could promote developmental brain disorders such as schizophrenia and ADHD.

Bibliography

584 Blankenship AG & Feller MB (2010) Mechanisms underlying spontaneous patterned

585 activity in developing neural circuits. Nat.Rev.Neurosci. 11:18–29.

586 Blin M, Norton W, Bally-Cuif L, Vernier P, Laure B-C & Vernier P (2008) NR4A2

587 controls the differentiation of selective dopaminergic nuclei in the zebrafish brain.

588 Molecular and cellular neurosciences 39:592–604.

589 Borodinsky LN, Root CM, Cronin JA, Sann SB, Gu X & Spitzer NC (2004) Activity-

590 dependent homeostatic specification of transmitter expression in embryonic

591 neurons. Nature 429:523–530.

592   Crepel V, Aronov D, Jorquera I, Represa A, Ben-Ari Y & Cossart R (2007) A

593   parturition-associated nonsynaptic coherent activity pattern in the developing

594   hippocampus. Neuron 54:105–120.

595   Demarque M, Represa A, Becq H, Khalilov I, Ben-Ari Y & Aniksztejn L (2002)

596   Paracrine intercellular communication by a Ca2+- and SNARE-independent

597   release of GABA and glutamate prior to synapse formation. Neuron 36:1051–

598   1061.

599   Demarque M & Spitzer NC (2010) Activity-Dependent Expression of Lmx1b

600   Regulates Specification of Serotonergic Neurons Modulating Swimming

601   Behavior. Neuron 67:321–334.

602   Dulcis D, Jamshidi P, Leutgeb S & Spitzer NC (2013) Neurotransmitter switching in

603   the adult brain regulates behavior. Science 340:449–453.

604   Dulcis D, Lippi G, Stark CJ, Do LH, Berg DK & Spitzer NC (2017) Neurotransmitter

605   Switching Regulated by miRNAs Controls Changes in Social Preference. Neuron

606   95:1319-1333.e5.

607   Dulcis D & Spitzer NC (2008) Illumination controls differentiation of dopamine

608   neurons regulating behaviour. Nature 456:195–201.

609   Dulcis D & Spitzer NC (2012) Reserve pool neuron transmitter respecification: Novel

610   neuroplasticity. Developmental Neurobiology 72:465–474.

611   Gawel K, Banono NS, Michalak A & Esguerra C V. (2019) A critical review of

612   zebrafish schizophrenia models: Time for validation? Neuroscience and

613   Biobehavioral Reviews 107:6–22.

614   Gomez TM, Robles E, Poo M & Spitzer NC (2001) Filopodial calcium transients

615   promote substrate-dependent growth cone turning. Science 291:1983–1987.

616   Gomez TM & Spitzer NC (1999) In vivo regulation of axon extension and pathfinding

617   by growth-cone calcium transients. Nature 397:350–355.

618   Klein MO, Battagello DS, Cardoso AR, Hauser DN, Bittencourt JC & Correa RG

619   (2019) Dopamine: Functions, Signaling, and Association with Neurological

620   Diseases. Cellular and Molecular Neurobiology 39:31–59.

621   Lange M, Froc C, Grunwald H, Norton WHJ & Bally-Cuif L (2018) Pharmacological

622   analysis of zebrafish lphn3.1 morphant larvae suggests that saturated

623   dopaminergic signaling could underlie the ADHD-like locomotor hyperactivity.

624   Progress in Neuro-Psychopharmacology and Biological Psychiatry 84:181–189.

625   Lange M, Norton W, Coolen M, Chaminade M, Merker S, Proft F, Schmitt A, Vernier

626   P, Lesch K-P & Bally-Cuif L (2012) The ADHD-linked gene Lphn3.1 controls

627   locomotor activity and impulsivity in zebrafish. Molecular psychiatry 17:855.

628   Ma PM (1994a) Catecholaminergic systems in the zebrafish. I. Number, morphology,

629   and histochemical characteristics of neurons in the locus coeruleus. Journal of

630   Comparative Neurology 344:242–255.

631   Ma PM (1994b) Catecholaminergic systems in the zebrafish. II. Projection pathways

632   and pattern of termination of the locus coeruleus. Journal of Comparative

633   Neurology 344:256–269.

634   Ma PM (1997) Catecholaminergic systems in the zebrafish. III. Organization and

635   projection pattern of medullary dopaminergic and noradrenergic neurons.

636   Journal of Comparative Neurology 381:411–427.

637   Ma PM (2003) Catecholaminergic systems in the zebrafish. IV. Organization and

638   projection pattern of dopaminergic neurons in the diencephalon. Journal of

639   Comparative Neurology 460:13–37.

640   Mandy M & Nyirenda M (2018) Developmental Origins of Health and Disease: the

641   relevance to developing nations. International health 10:66–70.

642   Murray RM, Bhavsar V, Tripoli G & Howes O (2017) 30 Years on: How the

643   Neurodevelopmental Hypothesis of Schizophrenia Morphed Into the

644   Developmental Risk Factor Model of Psychosis. Schizophrenia Bulletin 43:1190–

645   1196.

646   Owens DF & Kriegstein AR (1998) Patterns of intracellular calcium fluctuation in

647   precursor cells of the neocortical ventricular zone. Journal of Neuroscience

648   18:5374–5388.

649   Owens DF & Kriegstein AR (2002) Is there more to GABA than synaptic inhibition?

650   Nat.Rev.Neurosci. 3:715–727.

651   Plazas P V, Nicol N & Spitzer NC (2013) Activity-dependent competition regulates

652   motor neuron axon pathfinding via PlexinA3. Proceedings of the National

653   Academy of Sciences of the United States of America 110:1524–1529.

654   Scain AL, Le Corronc H, Allain AE, Muller E, Rigo JM, Meyrand P, Branchereau P &

655   Legendre P (2010) Glycine release from radial cells modulates the spontaneous

656   activity and its propagation during early spinal cord development. Journal of

657   Neuroscience 30:390–403.

658   Schweitzer J & Driever W (2009) Development of the dopamine systems in zebrafish.

659   Adv Exp Med Biol 651:1–14.

660   Schweitzer J, Löhr H, Filippi A & Driever W (2012) Dopaminergic and noradrenergic

661   circuit development in zebrafish. Developmental Neurobiology 72:256–268.

662   Spitzer NC, Kingston PA, Manning TJ & Conklin MW (2002) Outside and in:

663   development of neuronal excitability. Curr.Opin.Neurobiol. 12:315–323.

664   Tay TL, Ronneberger O, Ryu S, Nitschke R & Driever W (2011) Comprehensive

665   catecholaminergic projectome analysis reveals single-neuron integration of

666   zebrafish ascending and descending dopaminergic systems. Nature

667   Communications 2:112–171.

668   Warp E, Agarwal G, Wyart C, Friedmann D, Oldfield CS, Conner A, Del Bene F,

669   Arrenberg AB, Baier H, Isacoff EY, Bene F, Arrenberg AB, Baier H & Isacoff EY

670   (2012) Emergence of patterned activity in the developing zebrafish spinal cord.

671   Current Biology 22:93–102.

672   Yamamoto K, Ruuskanen JO, Wullimann MF & Vernier P (2011) Differential

673   expression of dopaminergic cell markers in the adult zebrafish forebrain. The

674   Journal of comparative neurology 519:576–598.

675

676

Figure legends

Figure 1 Presence of calcium spikes in the zebrafish telencephalon and their manipulations by transient balneation in pharmacological agents.

A. Consecutive images of a confocal time series of the brain of 48 hpf of Et(hsp:gal4;UAS:GCamp6f) embryos in control conditions. Fluorescence is displayed on a pseudocolor scale, the look up images intensity scale coding is shown in the right corner of the first image. Scale bar is 100µm. White dash circle surround the cell body of a cell displaying a calcium transient.

B. Changes in fluorescence intensity are plotted as a function of time. Ca2+ transients were scored for fluorescence changes, more than two times the SD of the baseline (dashed lines), and >3 sec in duration, calculated as the width at half-maximum. Representative traces from control conditions (in blue), following veratridine treatment (in green) and following treatment with a pharmacological cocktail containing TTX (2.5 µM), ω-Conotoxin (0.1 µM), Nifedipine (0.5 µM) and Flunarizine (2.5 µM) (TCNF, in red).

C. Left, boxplots showing the mean duration of single calcium spikes in control conditions (in blue, 3.3+/-1.6 sec), following veratridine treatment (in green, 3.7+/-1.7 sec) and following TCNF treatment (in red, 3.4+/-1.4 sec).

Middle, boxplots showing the mean frequency of calcium transients in control conditions (in blue, 6.6+/-5.4 spikes per hour, n=28 cells from 5 independent preparations), following veratridine treatment (in green, 9.2+/-6.6 spikes per hour, n=36 cells form 4 independent preparations) and following TCNF treatment (in red, 4.7+/-3 spikes per hour, n=17 cells form 4 independent preparations).

Right, boxplots showing the mean incidence of single calcium spikes in control conditions (in blue, 45.2+/-9.7%, n=5 independent preparations), following veratridine treatment (in green, 58.8+/-9.7%, n=4 independent preparations) and in the presence of TCNF (in red, 4.7+/-3 spikes per hour, n=17 cells form 4 independent preparations).

Figure 2 Effects of 24hrs balneation treatment on the number of dopaminergic neurons in the zebrafish larval telencephalon and OB.

A. Maximum projection of confocal z series of the brain of 6-7 dpf Et(VMAT2:eGFP) larvæ, in control conditions (left column boxed in blue), in the presence of veratridine (middle column, boxed in green) and in the presence of TCNF (right column, boxed in red). Immunostaining to TH (magenta) and GFP (cyan) and DAPI (yellow) are shown as merge and individual channels. Scale bars = 50 µm.

B-E. Boxplots showing the mean number of IR cells in control conditions, in the presence of veratridine and in the presence of "TCNF" in the telencephalon (B,C) and in the olfactory bulb (C,D), for TH (B,D) and for GFP (vMAT2 cells, C,E).

Figure 3 Absence of changes in cell death following increase or decrease of ENE

A. Maximum projection of confocal z series of the brain of 6-7 dpf Et(VMAT2:eGFP) larvæ, in control conditions (left image boxed in blue), in the presence of veratridine (middle image, boxed in green) and in the presence of TCNF (right image, boxed in red). Immunostaining to caspase-3 (magenta) and GFP (cyan) are shown as merged channels. Scale bars = 50 µm.

B. Boxplots showing the mean number of IR cells in control conditions, in the presence of veratridine and in the presence of "TCNF" for the caspase-3 staining in the olfactory bulb and the telencephalon.

Figure 4 Maturation of locomotion parameters

A-H. Boxplots showing the mean of 4 swimming parameters, number of episode (A,E), total duration (B,F), distance covered during swimming (C,G) and speed (D,H) for cruises episodes (A-D) and for bursts episodes (E-H) at different stage of larval development (4, 5, 6, and 7dpf).

Figure 5 Effects of 24hrs balneation treatments during embryonic development on spontaneous swimming of zebrafish larvæ.

A. Time line of the experiments indicating the timing (in days post fertilization, dpf) for the pharmacological treatments, and the following locomotion tests.

B. Representative path reconstructions for 24 individual larvæ during a 10 minutes trial for three experimental conditions. The portion of the path corresponding to bursts episodes (shown in red) are longer when early activity is increased (veratridine treatment) and shorter when early activity is decreased (T.C.N.F. treatment).

C-J. Boxplots showing the mean of different swimming parameters in different experimental conditions, Mean number of episode (C,G), total duration (D,H), distance covered during swimming (E,I) and speed (F,J) are shown for cruises episodes (C-F) and for bursts episodes (G-J).

Figure 6 Effects of 2hrs acute balneation treatments on zebrafish spontaneous swimming.

A-H. Boxplots showing the mean of different swimming parameters, mean number of episode (A,E), total duration (B,F), distance covered during swimming (C,G) and speed (D,H), for cruises episodes (A-D) and for bursts episodes (E-H), in different experimental conditions. The effects of 2hrs acute treatments with DMSO,

Veratridine, or TCNF are compared to pre-application recordings and 24hrs post-

application recordings.
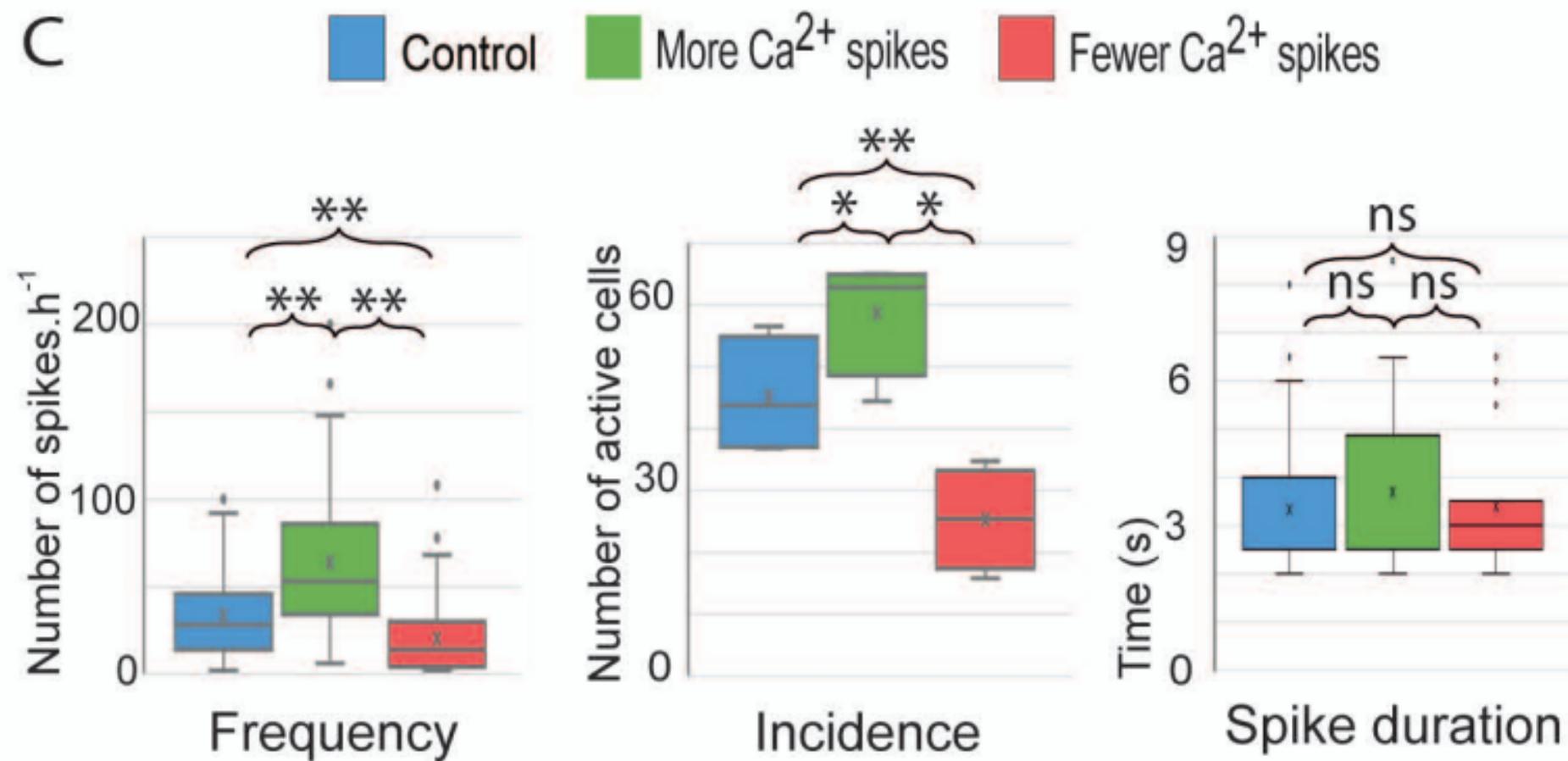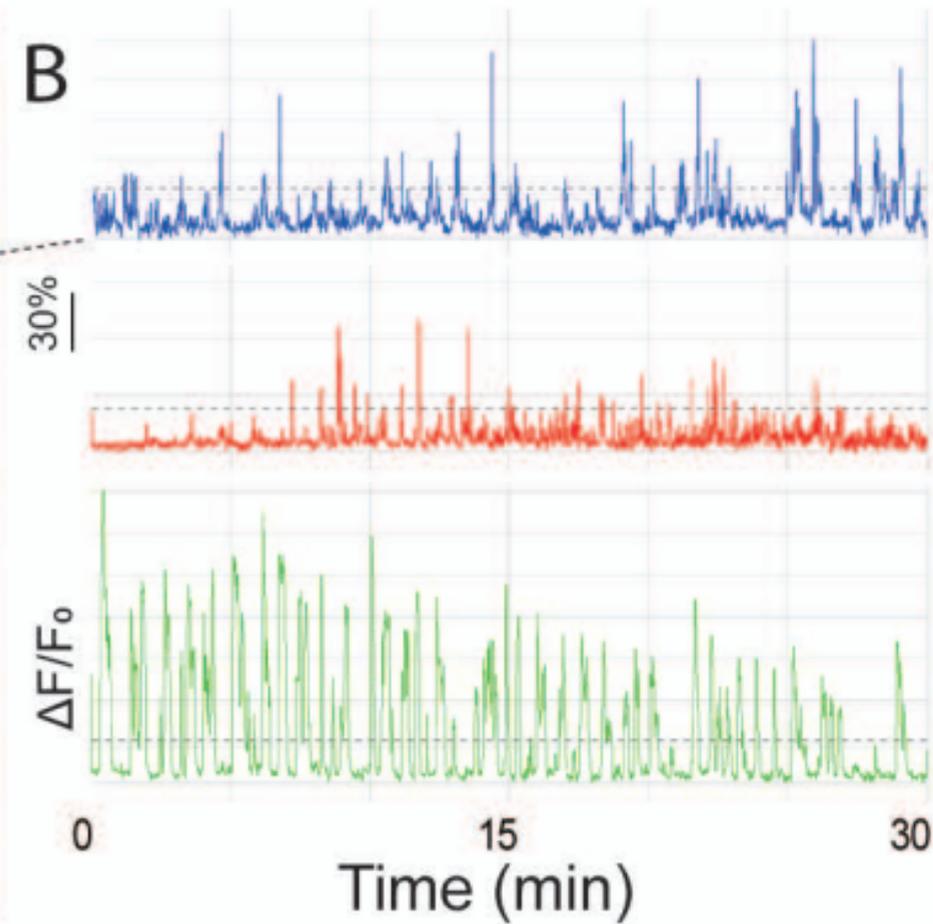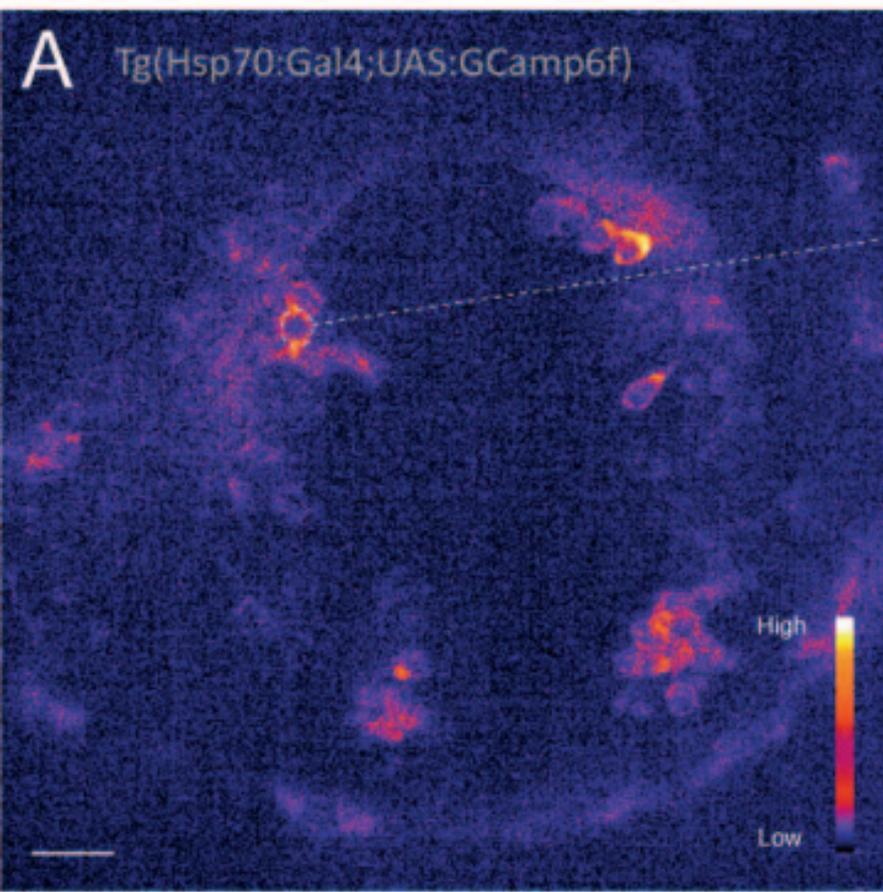
Bataille et al., Figure 1. Calcium spikes and their modulation by pharmacological treatments, in the embryonic zebrafish forebrain
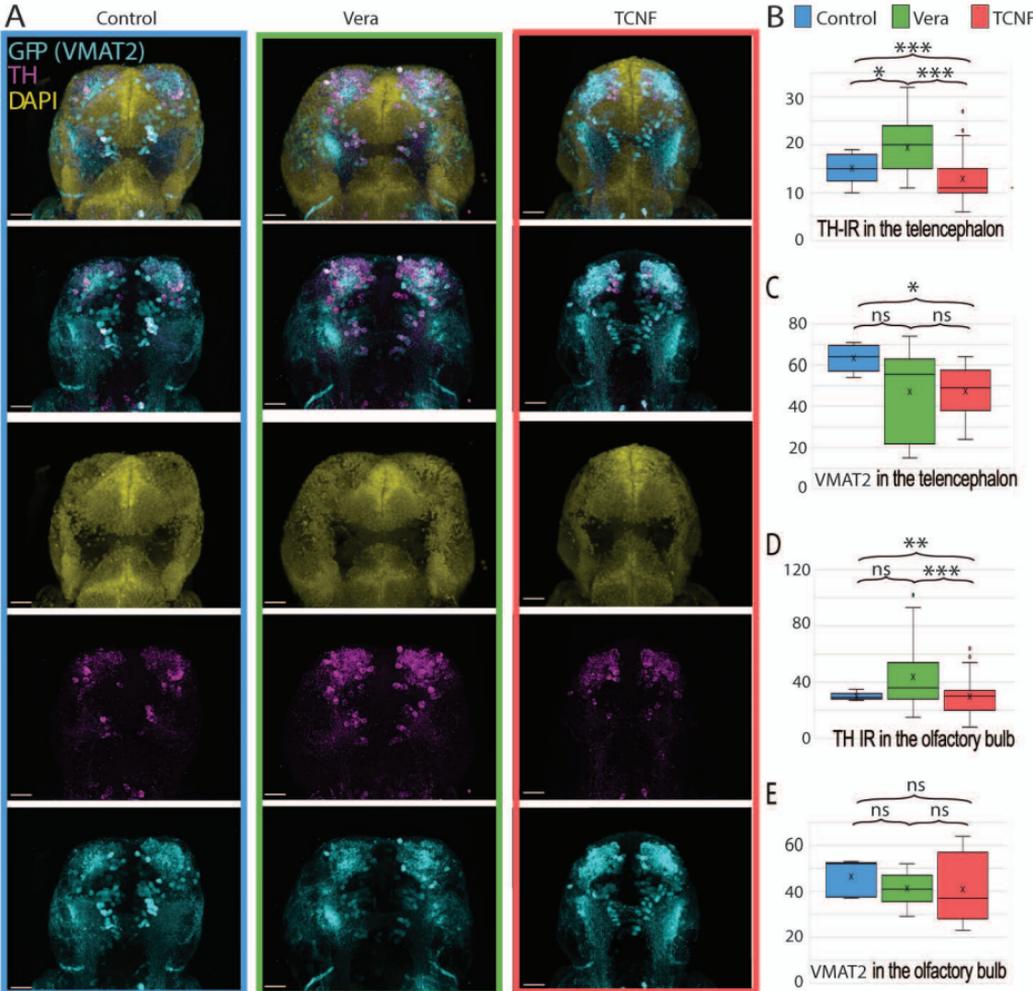
Bataille et al., Figure 2. Effects of ENE on the numbre of DA neurons in the zebrafish forebrain

A Control Veratridine TCNF

GFP (VMAT2)
Caspase 3

B

Caspase-3
in the telencephalon
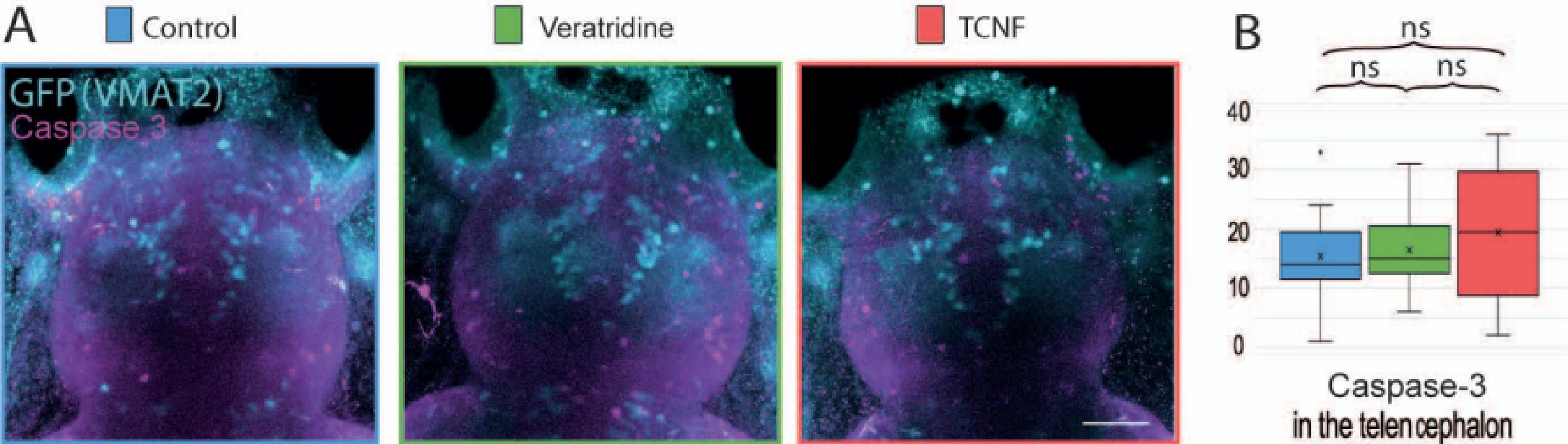
Bataille et al., Figure 3. Effects of ENE on caspase-3 expression in the larval zebrafish forebrain
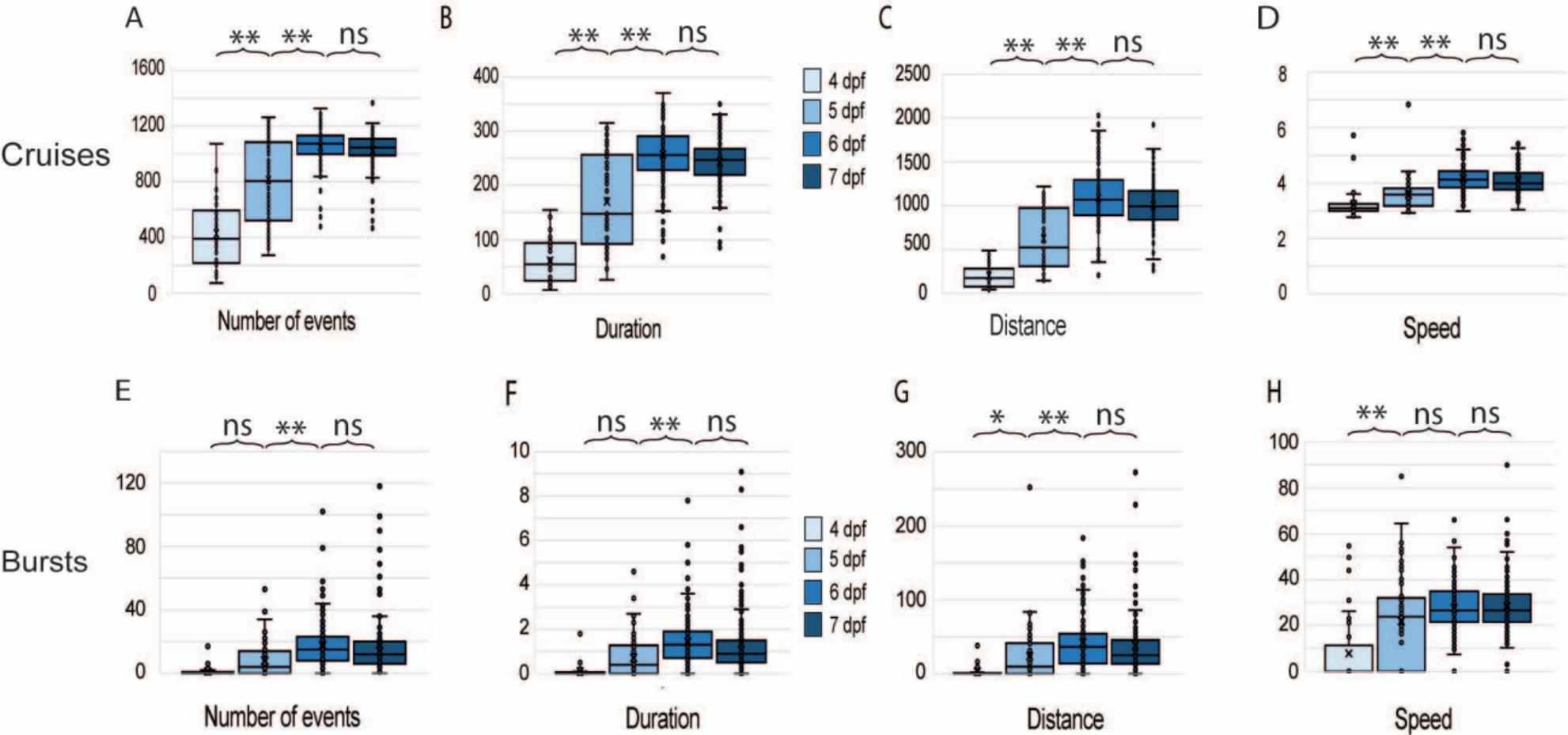
Bataille et al., Figure 4. Development of zebrafish spontaneous locomotion
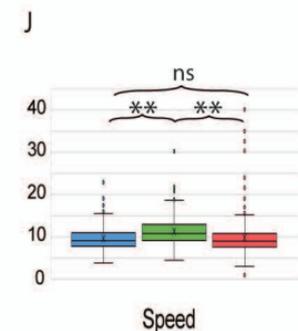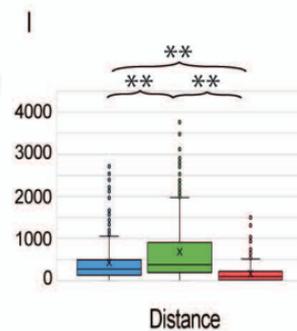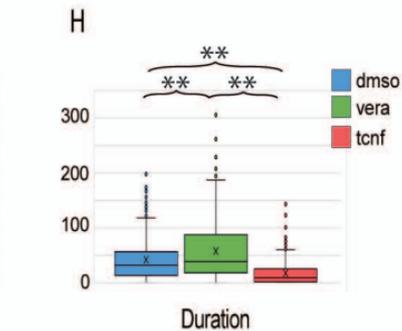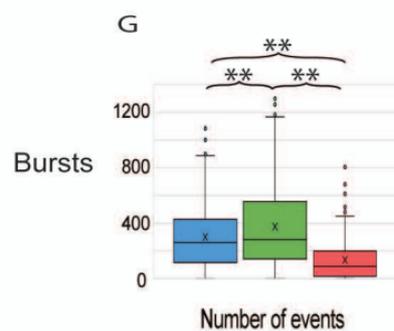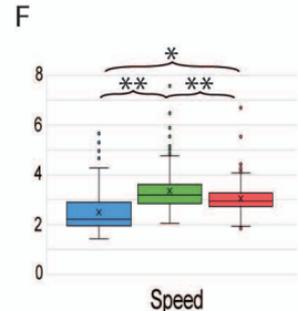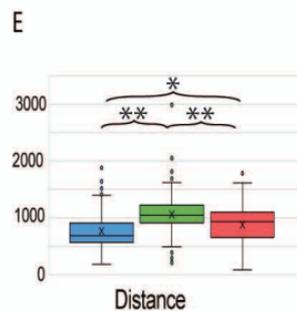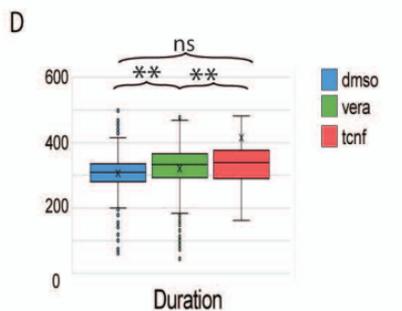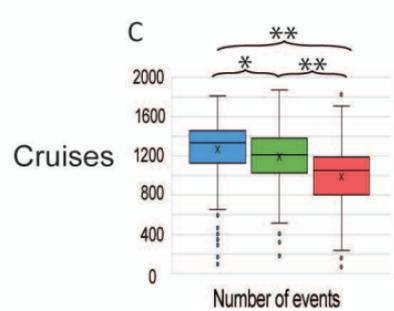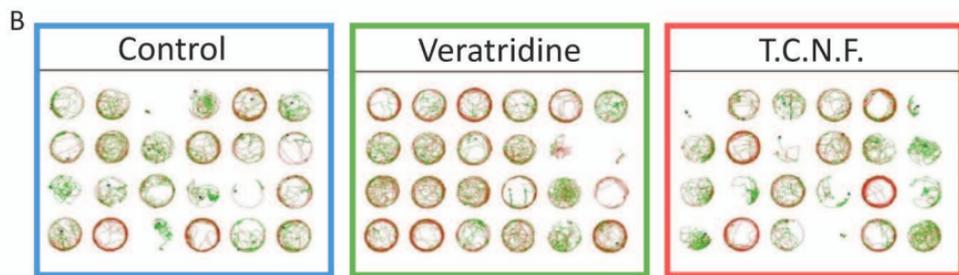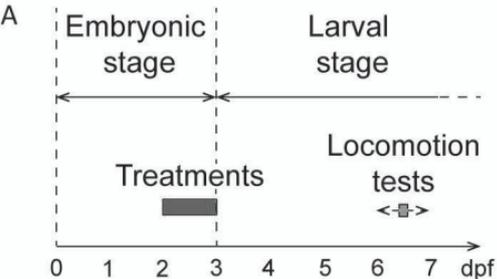
Bataille et al., Figure 5. Effects of ENE on the zebrafish spontaneous locomotion
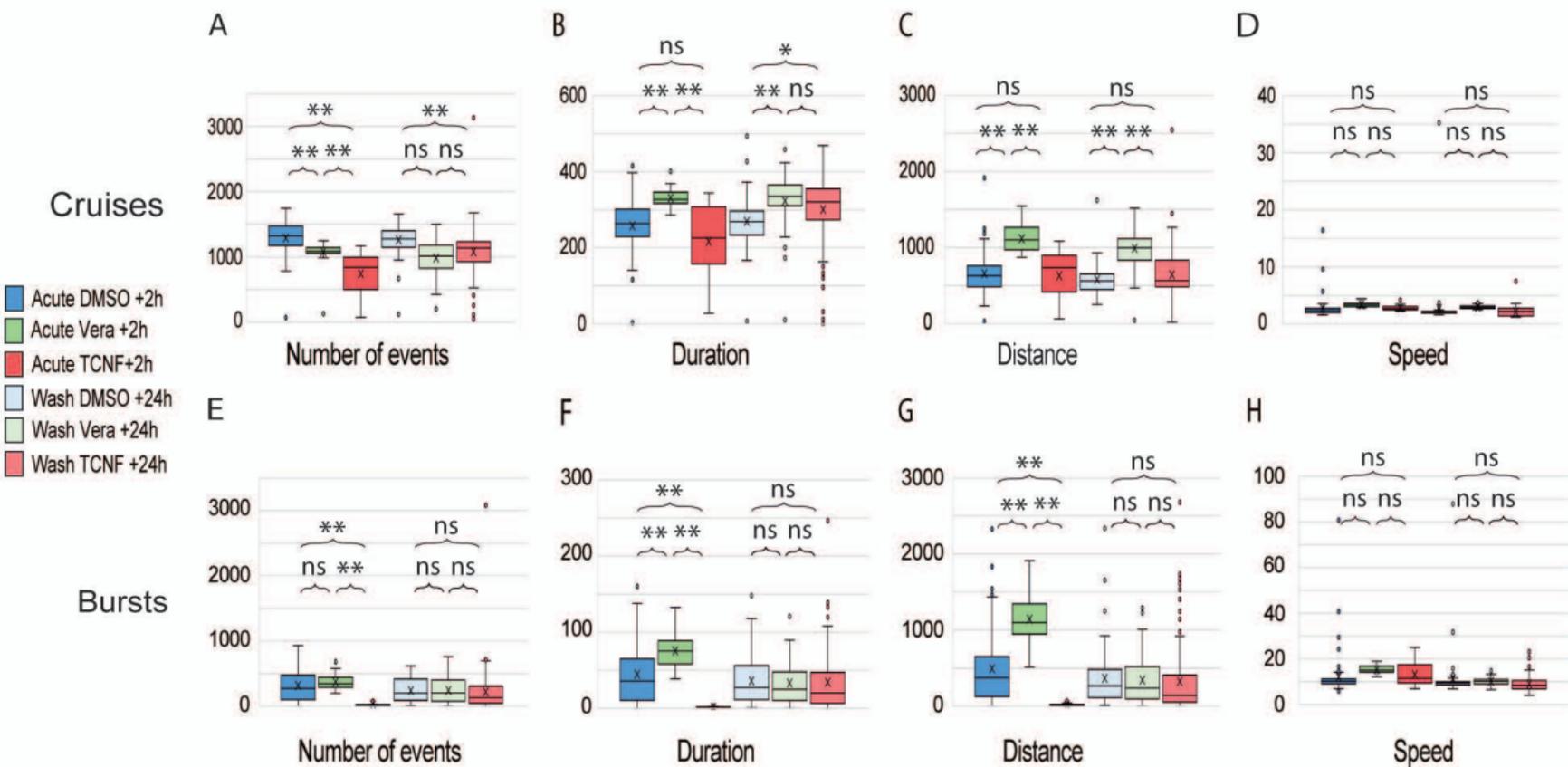
Bataille et al., Figure 6. Effects of acute pharmacological treatments on the zebrafish spontaneous locomotion